sciendo
10.2478/jlecol-2021-0017 Journal of Landscape Ecology (2021), **Vol: 14 / No. 3.**

ANALYSIS OF LAND USE LAND COVER CHANGES WITH LAND SURFACE TEMPERATURE USING SPATIAL-TEMPORAL DATA FOR NAGPUR CITY, INDIA

FARHAN KHAN[1], BHUMIKA DAS[2*], R. K. MISHRA[3] AND BRIJESH PATEL[4]

[1]*School of Engineering, Mats University, Raipur, Chhattisgarh, India.*
[2]*Department of Mining, Mats University, Raipur, Chhattisgarh, India.*
[3]*Bhilai Institute of Technology, Raipur, Chhattisgarh, India.*
[4]*Mats University, Raipur, Chhattisgarh, India.*
**Corresponding author email: drbhumika@matsuniversity.ac.in*

Received: 13th July 2021, **Accepted:** 16th August 2021

ABSTRACT

Remote sensing and Geographic Information System (GIS) are the most efficient tools for spatial data processing. This Spatial technique helps in generating data on natural resources such as land, forests, water, and their management with planning. The study focuses on assessing land change and surface temperature for Nagpur city, Maharashtra, for two decades. Land surface temperature and land use land cover (LULC) are determined using Landsat 8 and Landsat 7 imageries for the years 2000 and 2020. The supervised classification technique is used with a maximum likelihood algorithm for performing land classification. Four significant classes are determined for classification, i.e., barren land, built-up, vegetation and water bodies. Thermal bands are used for the calculation of land surface temperature. The land use land cover map reveals that the built-up and water bodies are increasing with a decrease in vegetation and barren land. Likewise, the land surface temperature map showed increased temperature for all classes from 2000 to 2020. The overall accuracy of classification is 98 %, and the kappa coefficients are 0.98 and 0.9 for the years 2000 and 2020, respectively. Due to urban sprawl and changes in land use patterns, the increase in land surface temperature is documented, which is a global issue that needs to be addressed.

Keywords: Nagpur, urban sprawl, land surface temperature, land use land cover, Kappa coefficient.

INTRODUCTION

Climate change caused by urban expansion is a result of worldwide population increase. Developing nations are therefore confronted with the additional issue of urbanization. When we discuss urbanization, the population plays an essential role in it. The global urban population is projected to rise from 55 % to 68 %, and this population growth will require land for their use (United Nations, 2018). 68 % of the total population of Nagpur District lives in an urban area, and 32 % lives in a rural area (Census, 2011). The alteration of LULC,

which has a significant impact on local, regional, and global environment, is one of the most conspicuous human modifications of terrestrial ecosystems (Mahmood *et al*., 2010; Mitsuda & Ito, 2011; Weng, 2001; Yu *et al*., 2011). For the past 150 years, annual temperatures have been rising continuously all across the world. However, different ground surfaces have different emissivity, temperature-bearing properties (Khan & Das, 2021; Sakhre *et al*., 2020). Some research shows that on a global scale, land and temperature changes have a negative impact on climatic conditions(Alves & L Skole, 1996). Rapid urbanization is depleting agricultural land, and the expansion of the metropolitan region leads towards various types of ground cover invasion, results in environmental deterioration. (Corner *et al*., 2014); (Chen *et al*., 2006). Many recent studies indicate that changes in LULC are a significant anthropogenic contributor to climate change because increasing urban activities are adversely affecting the environment (Kumar *et al*., 2017). Urban expansion affects the urban forest, water bodies, and vegetation (Dutta & Guchhait, 2020; Gazi *et al*., 2020; Mishra *et al*., 2020). The environmental changes due to LULC and LST is traced using spatial techniques, which will reduce the human effort of calculations (Akyürek *et al*., 2018). (Urgessa & Lemessa, 2020) states that, the land managers and conservationists should focus on the spatio-temporal changes occurring between various land use types and according to the changes the developing land use plans should be made. The current state of LULC transitions plays a vital role in controlling natural resources and tracking environmental changes; most of the city has been embedded in concrete as a result of urbanization, industrialization, and rapid population development (Sansare & Mhaske, 2020; Sansare & Mhaske, 2020). Land surface temperature (LST) is an essential parameter for surface energy balance and urban climatology studies. LST is influenced by land surface characteristics, including vegetation cover and form, land use-land cover, and surface imperviousness (Khandelwal *et al*., 2018; Yao *et al*., 2017; Peng *et al*., 2016). The more remarkable pattern shift in urban ground cover indicates that urbanization-induced land cover shifts affect the LST. In addition, temporal thermal signatures were generated and computed to show the LST trend corresponded to the major categories of LULC shifts in cities (Fu & Weng, 2016; Bokaie *et al.*, 2016; Zhou *et al.*, 2014).

The objective of the study

Because of the above, the current research uses an integrated method of remote sensing and GIS to investigate the effect of rapid urban development on LST in Nagpur, Maharashtra (India). The aim of the study is: (1) To determine LULC pattern and changes in the study period. (2) To generate LST from satellite imageries thermal bands for 2000 to 2020 (3) To determine the relationship between LULC and LST in the study area. This spatio-temporal analysis of urban environment and their relationship to LST may help with environmental management and planning in the study area.

MATERIALS AND METHODS

Study Area

Nagpur is the 3rd largest city after Mumbai and Pune in the state of Maharashtra. Nagpur is located at an altitude of 310 meters above mean sea level on the deccan plateau of the Indian peninsula, between 21° 2′ 59″ N to 21° 13′ 57″ N latitudes and 78° 59′ 29″ E to 78° 12′ 13″E longitudes. The area covered in the study is 217 km^2. It has a tropical rainy and dry atmosphere, with dry weather for most of the year. Nagpur has an average annual precipitation of 1000 to 1300 mm, with 80 percent of it coming during the monsoon season (Sakhre *et al*., 2020). Summers are scorching, march to June is the summer with May being

the hottest month of the year. November to January is the winter, and temperatures could go below 10°C. (50°f). The total population of Nagpur city according to census-2011 is 4,653,171, making it the ninth-largest urban city. Nagpur's population increased by 19.21 % in 2011 relative to 2001, according to the census. The study area map is shown in Fig. 1.

Fig. 1: Location map of the study area

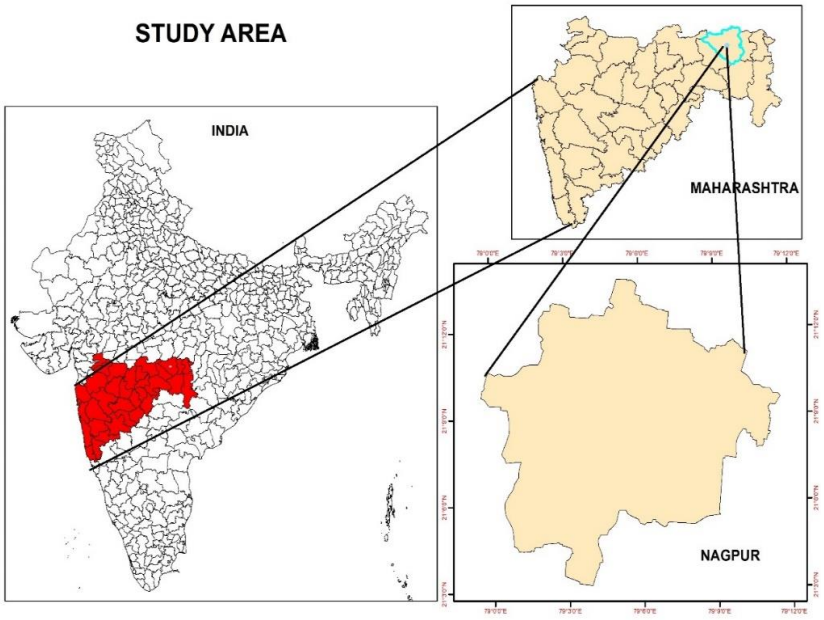

Data Collection

The data used for the study area analysis are (i) Landsat 7 thematic mapper images for the year 2000 dated 25 January 2000 and 14 April 2000. (ii) Landsat 8 OLI/TIRS images for 2020 dated 11 January 2020 and 16 April 2020 (Source: https://earthexplorer.usgs.gov). (iii) Google Earth Images for reference (source: Google Earth Pro) (iv) Nagpur urban boundary map (v) Topographic sheet of Nagpur of scale 1:250000 (source: Survey of India) (vi) ArcGIS 10.8 For Preparation of LST and LULC maps. (vii) The ground truth points are collected using Garmin trek 2.0 GPS for the same month corresponding to the satellite imagery used for 2020. The details about the Landsat images are given in Table **1**.

Table 1: Details of Land sat images used for the study

Producer	Sensor	Resolution	Cloud Cover	Date of Acquisition	Path/Row	Year
USGS	ETM	30mx30m	0.0	2000-04-17	144/045	2000
USGS	OLI_TIRS	30mx30m	0.0	2020-04-16	144/045	2020

Date in YY-MM-DD

Data Processing

Image Pre-processing

The satellite imageries used in this study were downloaded from the USGS site for different periods. The digital boundaries are created in ArcGIS (Khan *et al*., 2021) for processing further data. To obtain better results, the raster bands are pre-processed in ArcGIS software and image enhancement, atmospheric correction, removal of dark boundary and combining of different bands of images are done; this process is implemented for both the years 2000 and 2020. After successful pre-processing of satellite imageries, the area of interest is clipped for both the years, clipping reduces the image size.

Classification

The classification of all the images is performed in ArcGIS 10.8 using spatial analyst tool and maximum likelihood method of classification. The supervised classification method was selected for performing land use classification, in this method user trained the algorithm about different classes areas, this process is known as training sample which instruct the software to perform classification based on the trained samples. For classification, four classes are made (1) Vegetation, (2) Built-up, (3) barren land (4) water bodies. The ground verification was performed to verify the classes classified by the software. Using Global Positioning System, i.e., Garmin trek device, the ground verification is performed. The error matrix and kappa method were used to assess the mapping accuracy.

LST

The classified image of the study area is then used for the determination of LST. The LST map is generated using thermal band 6 for Landsat 7 and band 10, 11 for Landsat 8. Due to the high uncertainty, band 11 is not used in Landsat 8. The first step in LST retrieval is to use equation 1 for the TIRS sensor to transform the digital number (DN) of ground objects to spectral radiance (USGS, 2019)

$$L\lambda = ML * Qcal + AL - Oi \quad (1)$$

Where L_λ is spectral radiance in W/ (m^2 *sr * μm), M_L is the radiance multiplicative scaling factor for the band, q_{cal} is the level 1 pixel value in DN, and AL is an additive scaling factor for a band. O_i is the Calibration value for Landsat 8 TIRS band 10. The O_i value is 0.29 which is used in the study for calibration of Landsat image band 10 (USGS, 2017).

Secondly, atmospheric brightness temperature is derived from radiance, which is used for calculating LST. The calculation for deriving atmospheric brightness temperature is done using equation 2 (USGS, 2019).

$$T = \frac{K_2}{\mathrm{Ln}\left(\frac{K_1}{L_\lambda} + 1\right)} \quad (2)$$

T is the atmospheric brightness temperature in °K, K_1 and K_2 are the band-specific thermal conversion constant from metadata, and L_λ is the spectral radiance calculated in equation 1. The next step in calculating LST requires the calculation of normalised difference vegetation index (NDVI), proportion of vegetation (Pv) calculation of emissivity (ε) and then Finally, Land surface temperature is calculated. The equation used to generate the results are given below.

$$NDVI = (Band\ 4 - Band3)/(Band4 + Band3); \quad \text{(For Landsat 7 data)} \tag{3}$$

$$NDVI = (Band\ 5 - Band4)/(Band5 + Band4); \quad \text{(For Landsat 8 data)} \tag{4}$$

$$Pv = (\frac{NDVI - NDVI_{min}}{NDVI_{max} - NDVI_{min}})^2 \tag{5}$$

$$\varepsilon = mPv + n \tag{6}$$

$$LST = (T/(1 + (\lambda * \frac{T}{\rho}) \operatorname{Ln} \varepsilon \tag{7}$$

The normalized difference vegetation index is derived using equation 3, the proportion of vegetation (Pv) is calculated using the values obtained from NDVI calculation, maximum and minimum NDVI is used to calculate Pv using equation 5. The emissivity is calculated based on the value of Pv using equation 6, the value of m is taken as 0.004 and n value as 0.986 (Sobrino *et al*., 2004), and from all the above calculation LST is calculated using equation 7 where λ is 10.8μm wavelength of emitted radiance and ρ = h* c / σ = $1.438x10^{-2}$mk.

RESULTS

Land use Land Cover analysis using satellite imageries

From the analysis of different Landsat imageries, the land use cover classification is performed. The classification was based on the four classes; they are (1) Barren land, (2) Built-up area, (3) Vegetation (4) Water Bodies. The LULC images are shown in Fig. 2., and the analytical data is provided in Table 2. The land change matrix is shown in Table 3.

Table 2: LULC of Nagpur city

Land use land cover Classes	2000		2020		Change from 2000-2020	
	Km^2	%	Km^2	%	Km^2	%
Barren	61.55	27.55%	37.23	16.67%	-24.32	-10.88%
built-up	92.13	41.24%	151.59	67.86%	59.46	26.62%
Vegetation	67.4	30.17%	31.82	14.24%	-35.58	-15.93%
Water Bodies	2.33	1.04%	2.76	1.23%	0.43	0.19%

Table 3: Land change matrix (2000 to 2020)

Land Use Land Cover		2000			
		Barren	Built-Up	Vegetation	Water Bodies
2020	Barren	25.01	0.83	11.33	0
	Built-Up	30.14	89.69	31.65	0.01
	Vegetation	6.29	1.54	23.81	0.13
	Water Bodies	0.01	0.06	0.5	2.18

Fig. 2: LULC of 2000 and 2020

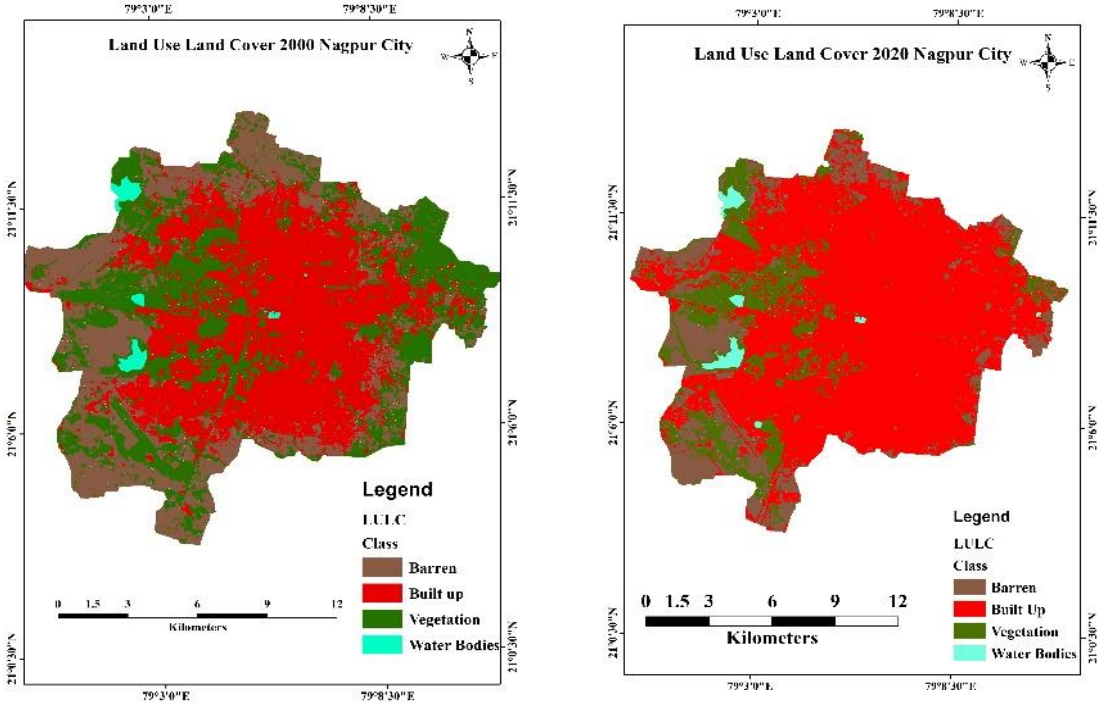

LST Analysis

The characteristics of the thermal signature for each LULC class was analyzed to understand the transition impact of LULC on radiant surface temperature. The LST map of Nagpur shows the surface temperature of different classes in Fig.3. The mean temperature change has been observed for different LULC classes shown in Table 4 and temperature change from 2000 to 2020 is given in Table 5. The LST images for built-up areas are given in Fig. 4.

Fig. 3: LST for Nagpur City (2000 to 2020)

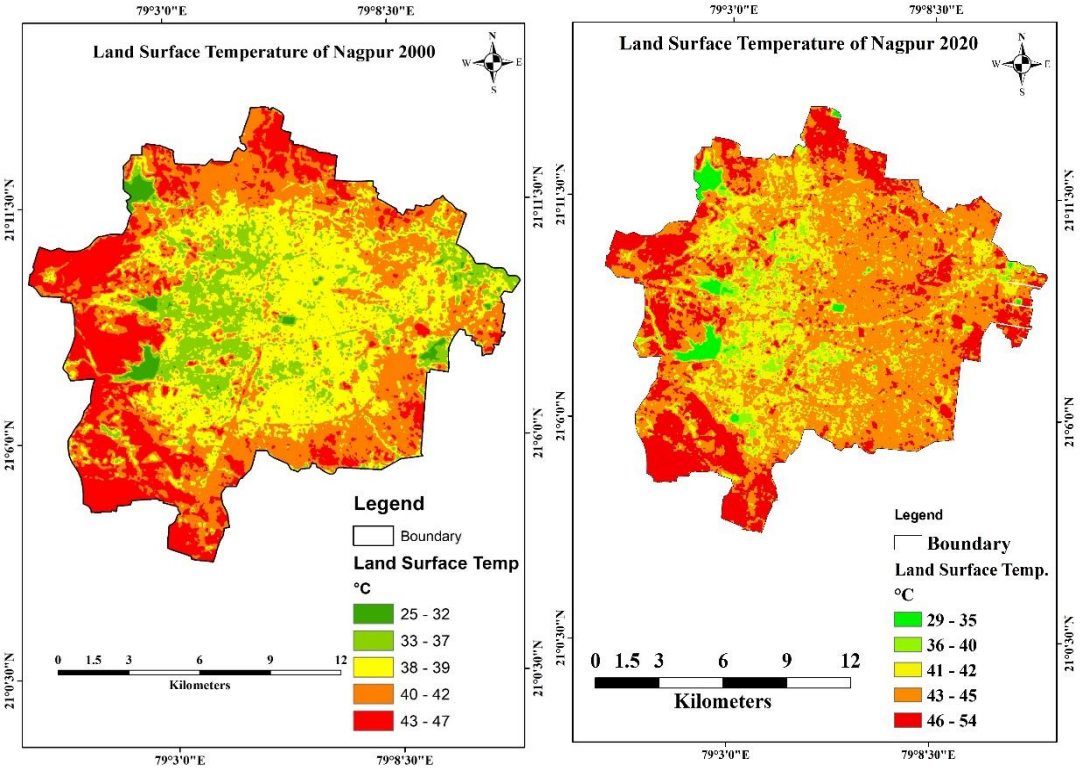

Table 4: Mean LST of Study area (2000 to 2020)

LULC Classes	Mean LST in degree Celsius (°C)	
	2000	2020
Barren	42.6	46.48
built-up	38.48	43.02
Vegetation	33.88	41.87
Water Bodies	27.45	30.75

Table 5: Temperature Change (2000 to 2020)

	Temperature	2000	2020	Change (2000 to 2020)
Class	Barren	42.6	46.48	+3.88
	Built-Up	38.48	43.02	+4.54
	Vegetation	33.88	41.87	+2.99
	Water Bodies	27.45	30.75	+3.3

Fig. 4: LST for Built-Up (2000 to 2020)

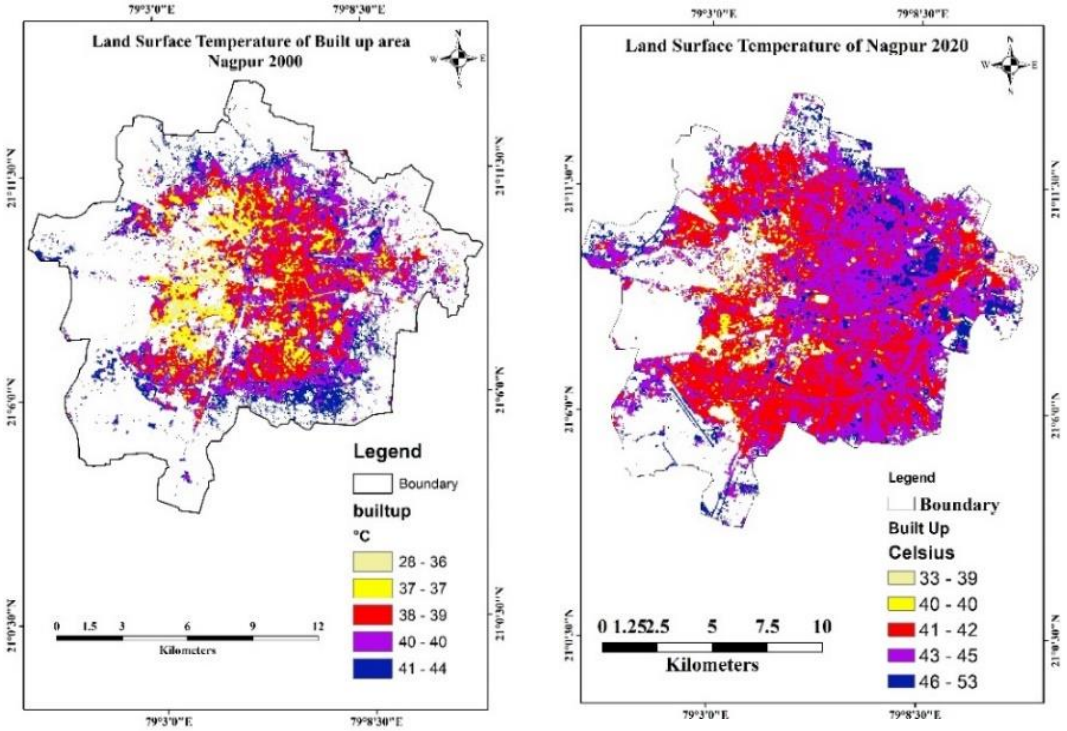

Accuracy assessment

The accuracy assessment is essential to determine the user and producer efficiency during classification. The overall accuracy is found to be 98 % for both the year. The kappa Coefficients are 0.98 and 0.9 for the years 2000 and 2020 respectively.

DISCUSSION

Land Use land cover

The analysis reveals that in the year 2000, the area covered under barren land was about 27.55 % (61.55 km^2), 41.24 % (92.13 km^2) area under built-up land, 30.17 % (67.4 km^2) area under vegetation, and water bodies covered 1.04 % (2.33 km^2) area. Similarly, in the year 2020, the area covered by barren land is 16.67 % (37.23 km^2), 67.86 % (151.59 km^2) for built-up land, 14.24 % (31.82 km^2) for vegetation and 1.23 % (2.76 km^2) for water bodies. During Image classification, there may be chances of uncertainty due to visual interpretation of areas(Brus *et al*., 2018).

An initial objective of the study is to identify factors driving land changes. Result shows, the changes mainly occurred between two classes of built-up and vegetation. The built-up area increased by about 26.62 % (59.46 km^2) of the total area, vegetation is decreased by 15.93 % (35.58 km^2), barren land is also decreased by 10.88% (24.32 km^2), and water bodies increased by 0.19 % (0.43 km^2) of the total study area.

The present study aims to determine the land use cover and determine the changes in landform for the last two decades, a land change matrix is generated. The land change matrix

reveals that during 2000 to 2020, about 30.14 km^2 area of barren land is changed to built-up region, 6.29 km^2 area to vegetation and 0.01 km^2 area is converted to water bodies; about 11.33 km^2 area of vegetation is converted to barren, 31.65 km^2 area converted to built-up and 0.5 km^2 area to water bodies; about 0.01 km^2 area of water bodies is converted to built-up and 0.13 km^2 area to vegetation. The loss of 31.65 km^2 of the existing forest cover is due to urban growth. The reduction of forest cover due to urbanization has a significant effect on the region's environmental sustainability (Sahana *et al*., 2016).

LST

The LST shows the barren land and built-up both have the highest temperature in the study area, barren has 42.6 °C in 2000, and 46.48 °C in 2020, the built-up area shows a temperature of 38.48°C in 2000 and 43.02 °C in 2020. Results shows that both classes of land use contribute to the rising temperature of the study area. It means that by replacing natural vegetation with non-evaporating, non-transpiring surfaces like stone, metal, and concrete, urban construction increases surface radiant temperature (Fonseka *et al*., 2019; Yuan & Bauer, 2007). The temperature for vegetation area is 33.88°C in 2000 and 41.87°C in 2020. The lowest surface temperature is observed for the water bodies, 27.45°C in 2000 and 30.75 °C in 2020.

The change in LST from the year 2000 to 2020, barren land is increased by 3.88°C, for built-up/urban it is increased by 4.54°C, for the vegetation-covered area it is increased by 2.99°C, and for water bodies, the surface temperature is increased by 3.3°C.

LST for built-up area

The built-up area is studied separately to determine the effect of urban development on LST (Fig. 4). The built-up area polygon is reprocessed in ArcGIS, and the database for built-up was generated. The variation of LST and change across the city are analysed. From Fig. 4., the changes are observed. For the year 2000, the LST of built-up area is having max temperature 40°C to 44°C, while in the year 2020, the max temperature increases by 41°C to 53°C, which is noticeable. From the above Fig. 4., the urban growth is perceived, and due to urban expansion activities, the surface radiance is increased in the urban areas (Das *et al*., 2021; Fonseka *et al*., 2019; Ghosh *et al*., 2019; Khandelwal *et al*., 2018).

CONCLUSION

The objective of the study is to determine qualitative and quantitative results for LULC and LST. The study is performed for a period of twenty years, from 2000 to 2020. The study also focuses on using GIS and remote sensing for the assessment of LST and LULC. The study explains that the rapid changes in land affects the temperature, which is a critical issue. Another aspect of the study suggests that policymakers for environment conservation should make policies that can prohibit the land change issue in the study area. The central part of the built-up area shows more negligible effect on temperature change due to urban forest area, as compared to outer part of the study area because government bodies may not maintain the outer parts, results in temperature increase due to deforestation.

The conclusion of the complete study is stated below:

(i) LULC and LST are directly proportional to each other; as the land is mismanaged, the temperature will be increased. The study was compiled of LULC analysis, LST analysis followed by LST for built-up.

(ii) The remote sensing and GIS data results show the rapid growth in the urban area, with a decrease in vegetation and water bodies. The acceleration of economic development is the source of urbanization. The mean LST over the area has been consistently increasing over the years, indicating that the city will see more summer heat in the coming years. If more temperature-bearing surfaces take natural ones, the rise in LST is closely associated with substantial urbanization in the region.

(iii) The negative association was discovered between mean LST and vegetation, indicating that vegetation would help in reducing LST in the city.

(iv) The result from the study shows, for LULC total area was 223.4 sq. km, due to changes the increase of 59.46 sq. km of built-up area and 0.43 sq. km of water bodies are observed with a decrease in 24.32 sq. km of barren land and 35.58 sq. km of vegetation area. The LULC change results also show that 30.14 sq. km area of barren land and 31.65 sq. km of vegetation land is converted into the built-up area.

(v) Similarly, for LST results shows that for the year 2000, the mean built-up area temperature was 38.48°C and 42.6°C for barren land, for the year 2020, the temperature of both the classes increase to 43.02°C and 46.48 °C, respectively. The average temperature increase for twenty years is about 3.67°C.

The study will attract international researchers and national researchers because the temperature change issue is global, and the results of land change and surface temperature may be correlated with the findings of the study to better understand land cover influences the temperature. The exciting fact determined in the study is that the government bodies only work for city areas, which results in controlled temperature, but the outer parts are not maintained, resulting in increased temperature.

CONFLICTS OF INTEREST

The authors declare no conflict of interest.

REFERENCES

Akyürek, D., Koç, Ö., Akbaba, E. M., & Sunar, F. (2018). Land Use/Land Cover Change Detection Using Multi–Temporal Satellite Dataset: A Case Study in Istanbul New Airport. *ISPRS - International Archives of the Photogrammetry, Remote Sensing and Spatial Information Sciences*, *XLII-3/W4*, 17-22. https://doi.org/10.5194/isprs-archives-XLII-3-W4-17-2018

Alves, D. S., & L Skole, D. (1996). Characterizing land cover dynamics using multi-temporal imagery. *International Journal of Remote Sensing*, *17*(4), 835-839. https://doi.org/10.1080/01431169608949049

Bokaie, M., Zarkesh, M. K., Arasteh, P. D., & Hosseini, A. (2016). Assessment of Urban Heat Island based on the relationship between land surface temperature and Land Use/ Land Cover in Tehran. *Sustainable Cities and Society*, *23*, 94-104. https://doi.org/https://doi.org/10.1016/j.scs.2016.03.009

Brus, J., Pechanec, V., & Machar, I. (2018). Depiction of uncertainty in the visually interpreted land cover data. *Ecological Informatics*, *47*, 10-13. https://doi.org/10.1016/j.ecoinf.2017.10.015

Census. (2011). *DistrictCensusHandbook (DCHB)*.

Chen, X.-L., Zhao, H.-M., Li, P.-X., & Yin, Z.-Y. (2006). Remote sensing image-based analysis of the relationship between urban heat island and land use/cover changes. *Remote Sensing of Environment*, *104*(2), 133-146. https://doi.org/https://doi.org/10.1016/j.rse.2005.11.016

Corner, R. J., Dewan, A. M., & Chakma, S. (2014). Monitoring and Prediction of Land-Use and Land-Cover (LULC) Change. In A. Dewan & R. Corner (Eds.), *Dhaka Megacity: Geospatial Perspectives on Urbanisation, Environment and Health* (pp. 75-97). Springer Netherlands. https://doi.org/10.1007/978-94-007-6735-5_5

Das, N., Mondal, P., Sutradhar, S., & Ghosh, R. (2021). Assessment of variation of land use/land cover and its impact on land surface temperature of Asansol subdivision. *The Egyptian Journal of Remote Sensing and Space Science*, *24*(1), 131-149. https://doi.org/https://doi.org/10.1016/j.ejrs.2020.05.001

Dutta, S., & Guchhait, S. K. (2020). Assessment of land use land cover dynamics and urban growth of Kanksa Block in Paschim Barddhaman District, West Bengal. *GeoJournal*. https://doi.org/10.1007/s10708-020-10292-3

Fonseka, H. P. U., Zhang, H., Sun, Y., Su, H., Lin, H., & Lin, Y. (2019). Urbanization and Its Impacts on Land Surface Temperature in Colombo Metropolitan Area, Sri Lanka, from 1988 to 2016. *Remote Sensing*, *11*(8), 957. https://www.mdpi.com/2072-4292/11/8/957

Fu, P., & Weng, Q. (2016). A time series analysis of urbanization induced land use and land cover change and its impact on land surface temperature with Landsat imagery. *Remote Sensing of Environment*, *175*, 205-214. https://doi.org/https://doi.org/10.1016/j.rse.2015.12.040

Gazi, M. Y., Rahman, M. Z., Uddin, M. M., & Rahman, F. M. A. (2020). Spatio-temporal dynamic land cover changes and their impacts on the urban thermal environment in the Chittagong metropolitan area, Bangladesh. *GeoJournal*. https://doi.org/10.1007/s10708-020-10178-4

Ghosh, S., Chatterjee, N. D., & Dinda, S. (2019). Relation between urban biophysical composition and dynamics of land surface temperature in the Kolkata metropolitan area: a GIS and statistical based analysis for sustainable planning. *Modeling Earth Systems and Environment*, *5*(1), 307-329. https://doi.org/10.1007/s40808-018-0535-9

Khan, F., & Das, B. (2021, 2021/06/01). *Geospatial approach to determine Soil bearing capacity of Nagpur city, Maharashtra India* IOP Conference Series: Earth and Environmental Science, http://dx.doi.org/10.1088/1755-1315/796/1/012069

Khan, F., Das, B., Ram Krishna Mishra, S., & Awasthy, M. (2021). A review on the Feasibility and Application of Geospatial Techniques in Geotechnical Engineering Field. *Materials Today: Proceedings*. https://doi.org/https://doi.org/10.1016/j.matpr.2021.02.108

Khandelwal, S., Goyal, R., Kaul, N., & Mathew, A. (2018). Assessment of land surface temperature variation due to change in elevation of area surrounding Jaipur, India. *The Egyptian Journal of Remote Sensing and Space Science*, *21*(1), 87-94. https://doi.org/https://doi.org/10.1016/j.ejrs.2017.01.005

Kumar, M., Tripathi, D. K., Maitri, V., & Biswas, V. (2017). Impact of Urbanisation on Land Surface Temperature in Nagpur, Maharashtra. In P. Sharma & S. Rajput (Eds.), *Sustainable Smart Cities in India: Challenges and Future Perspectives* (pp. 227-241). Springer International Publishing. https://doi.org/10.1007/978-3-319-47145-7_15

Mahmood, R., Pielke, R. A., Hubbard, K. G., Niyogi, D., Bonan, G., Lawrence, P., McNider, R., McAlpine, C., Etter, A., Gameda, S., Qian, B., Carleton, A., Beltran-Przekurat, A., Chase, T., Quintanar, A. I., Adegoke, J. O., Vezhapparambu, S., Conner, G., Asefi, S., Sertel, E., Legates, D. R., Wu, Y., Hale, R., Frauenfeld, O. W., Watts, A., Shepherd, M., Mitra, C., Anantharaj, V. G., Fall, S., Lund, R., Treviño, A., Blanken, P., Du, J., Chang, H.-I., Leeper, R., Nair, U. S., Dobler, S., Deo, R., & Syktus, J. (2010). Impacts of Land Use/Land Cover Change on Climate and Future Research Priorities. *Bulletin of the American Meteorological Society*, *91*(1), 37-46. https://doi.org/10.1175/2009bams2769.1

Mishra, P. K., Rai, A., & Rai, S. C. (2020). Land use and land cover change detection using geospatial techniques in the Sikkim Himalaya, India. *The Egyptian Journal of Remote Sensing and Space Science*, *23*(2), 133-143. https://doi.org/10.1016/j.ejrs.2019.02.001

Mitsuda, Y., & Ito, S. (2011). A review of spatial-explicit factors determining spatial distribution of land use/land-use change. *Landscape and Ecological Engineering*, *7*(1), 117-125. https://doi.org/10.1007/s11355-010-0113-4

Peng, J., Xie, P., Liu, Y., & Ma, J. (2016). Urban thermal environment dynamics and associated landscape pattern factors: A case study in the Beijing metropolitan region. *Remote Sensing of Environment*, *173*, 145-155. https://doi.org/https://doi.org/10.1016/j.rse.2015.11.027

Sahana, M., Ahmed, R., & Sajjad, H. (2016). Analyzing land surface temperature distribution in response to land use/land cover change using split window algorithm and spectral radiance model in Sundarban Biosphere Reserve, India. *Modeling Earth Systems and Environment*, *2*(2), 81. https://doi.org/10.1007/s40808-016-0135-5

Sakhre, S., Dey, J., Vijay, R., & Kumar, R. (2020). Geospatial assessment of land surface temperature in Nagpur, India: an impact of urbanization. *Environmental Earth Sciences*, *79*(10), 226. https://doi.org/10.1007/s12665-020-08952-1

Sansare, D. A., & Mhaske, S. Y. (2020). Land use change mapping and its impact on storm water runoff using Remote sensing and GIS: a case study of Mumbai, India. *IOP Conference Series: Earth and Environmental Science*, *500*, 012082. https://doi.org/10.1088/1755-1315/500/1/012082

Sansare, D. A., & Mhaske, S. Y. (2020). Natural hazard assessment and mapping using remote sensing and QGIS tools for Mumbai city, India. *Natural Hazards*, *100*(3), 1117-1136. https://doi.org/10.1007/s11069-019-03852-5

Sobrino, J. A., Jiménez-Muñoz, J. C., & Paolini, L. (2004). Land surface temperature retrieval from LANDSAT TM 5. *Remote Sensing of Environment*, *90*(4), 434-440. https://doi.org/https://doi.org/10.1016/j.rse.2004.02.003

United Nations. (2018). *World Urbanization Prospects: The 2018 Revision, Methodology*. (ESA/P/WP.252). Retrieved December 8, 2020, from https://population.un.org/wup/Publications/Files/WUP2018-Methodology.pdf

Urgessa, T., & Lemessa, D. (2020). Spatiotemporal Landuse Land Cover Changes in Walmara District, Central Oromia, Ethiopia. *Earth Sciences*, *9*(1). https://doi.org/10.11648/j.earth.20200901.14

USGS. (2017). *Landsat 8 OLI and TIRS Calibration Notices.* Retrieved December 8, 2020, from https://www.usgs.gov/core-science-systems/nli/landsat/landsat-8-oli-and-tirs-calibration-notices

USGS. (2019). *Landsat 8 (L8)Data Users Handbook* (Vol. version 5). USGS.

Weng, Q. (2001). A remote sensing?GIS evaluation of urban expansion and its impact on surface temperature in the Zhujiang Delta, China. *International Journal of Remote Sensing*, *22*(10), 1999-2014. https://doi.org/10.1080/713860788

Yao, R., Wang, L., Huang, X., Niu, Z., Liu, F., & Wang, Q. (2017). Temporal trends of surface urban heat islands and associated determinants in major Chinese cities. *Science of The Total Environment*, *609*, 742-754. https://doi.org/https://doi.org/10.1016/j.scitotenv.2017.07.217

Yu, W., Zang, S., Wu, C., Liu, W., & Na, X. (2011). Analyzing and modeling land use land cover change (LUCC) in the Daqing City, China. *Applied Geography*, *31*(2), 600-608. https://doi.org/https://doi.org/10.1016/j.apgeog.2010.11.019

Yuan, F., & Bauer, M. E. (2007). Comparison of impervious surface area and normalized difference vegetation index as indicators of surface urban heat island effects in Landsat imagery. *Remote Sensing of Environment*, *106*(3), 375-386. https://doi.org/https://doi.org/10.1016/j.rse.2006.09.003

Zhou, D., Zhao, S., Liu, S., Zhang, L., & Zhu, C. (2014). Surface urban heat island in China's 32 major cities: Spatial patterns and drivers. *Remote Sensing of Environment*, *152*, 51-61. https://doi.org/https://doi.org/10.1016/j.rse.2014.05.017